



THE 13TH VIENNA CONFERENCE ON INSTRUMENTATION

11 - 15 February 2013

14 Feb 2013 | Vienna University of Technology

Session: Medical Applications

Presented by **Jorge A. NEVES**

Development and Performance Evaluation of a Simultaneous PET-MR Detector based on the ClearPEM Technology



The ClearPEM breast imaging scanner

Jorge A. Neves

Laboratório de Instrumentação e Física Experimental de Partículas (LIP), Lisbon, Portugal

On behalf of the ClearPEM Collaboration

ARTICLE INFO

Available online 6 July 2010

Keywords:

Positron emission mammography
Avalanche photodiodes
Front-end electronics
Application-Specific Integrated Circuit (ASIC)
Energy and time resolution
Image reconstruction

ABSTRACT

We present results on the characterization of the ClearPEM breast imaging scanner. ClearPEM is a dual-head positron emission mammography scanner using APD-based detector modules that are capable of measuring the depth-of-interaction (DOI) with a resolution of 2 mm in LYSO:Ce crystals. The full system comprises 192 detector modules with a total of 6144 LYSO:Ce crystals and 384 32-pixel APD arrays read out by ASICs with 192 input channels. The scanner includes front-end and data acquisition electronics and a robotic gantry for detector placement and rotation. The software implements calibration (energy, time and DOI), normalization and image reconstruction algorithms.

In this conference, the scanner main technical characteristics, the calibration strategies and the spectrometric performance in clinical environment were presented as well as the images obtained with point sources and with a microDerenzo phantom. The image resolution was found to be of the order of 1.3 mm FWHM (center of field-of-view) and the DOI capability has shown to have a strong impact on the image sharpness. An assessment of the first clinical experience was also presented at the conference.

© 2010 Elsevier B.V. All rights reserved.

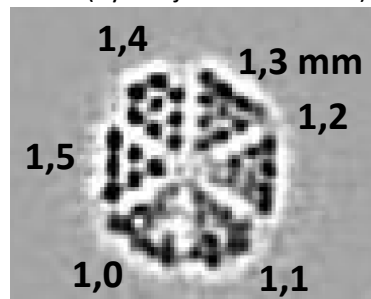
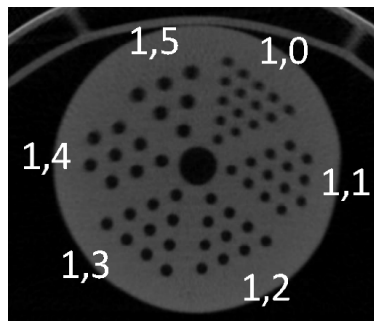
1. Introduction

Breast cancer is the most common cancer affecting women, with an incidence rate of about 1.2 million females per year worldwide. Positron emission tomography has demonstrated large potential for cancer detection since the radiotracer injected into the patient fixates in tumor cells and its biodistribution can be measured by the temporal coincidence detection of the 2γ photons resulting from the positron-electron annihilation when the radiotracer decays. Here is presented the ClearPEM—a breast cancer imaging scanner developed by the Portuguese PET consortium under the framework of the Crystal Clear Collaboration [1].

interaction coordinate along 20 mm crystals with a resolution of 2 mm FWHM [2]. This reduces the degradation of the spatial resolution due to the parallax effect, in particular when the scanner operates at smaller separation distance between the detectors (8–10 cm) in order to increase the photon detection acceptance. We had investigated the influence of the DOI resolution on reconstructed images using simulated data and had concluded that a 2 mm DOI resolution allows to achieve an image spatial resolution of about 1.2 mm [1].

The detector module consists on 32 LYSO:Ce crystals with $2 \times 2 \times 20 \text{ mm}^3$ arranged on a 4×8 matrix made of BaSO_4 walls. It is optically coupled on both ends to APD arrays that can be assembled in a planar arrangement within the detector heads.

CT and ClearPEM images of a Bioscan mini-Jaszczak phantom (by Benjamin A. FRISCH)



ClearPEM - Detection and Imaging Performance

Energy Resolution

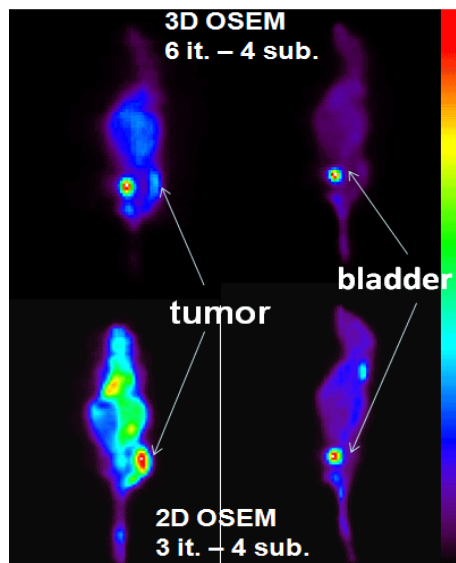
13.3% @ 511 keV (FWHM)

Time Resolution

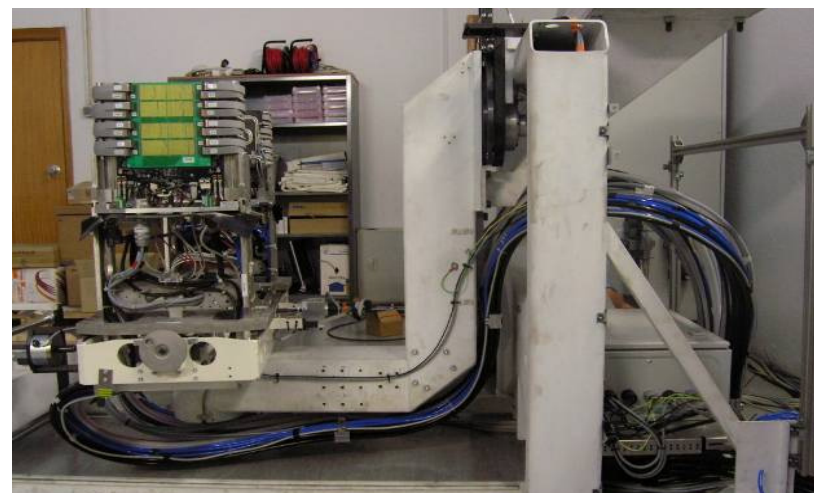
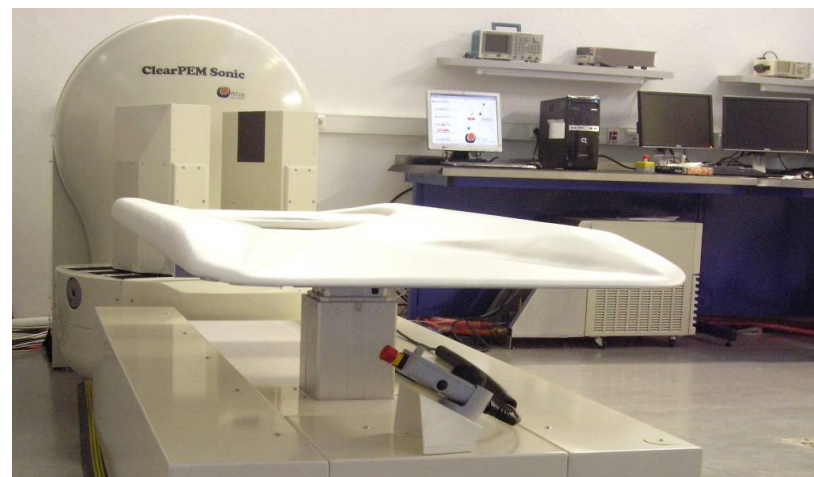
4.47 ns (FWHM)

Spatial Resolution

< 1.3 mm (FWHM)



Small-animal imaging



ClearPEM-Sonic (2nd prototype - Lisbon, 2011)



“Do not try to develop a PET-MR prototype before build your own PET scanner first...”

Outline

1. *Motivations for Combined PET-MR Imaging*
2. *Electromagnetic Compatibility Issues*
3. *CIBM/ EPFL Magnet Facility*
4. *ClearPEM Detectors & Front-end Electronics*
5. *Mutual Electromagnetic Interference Tests*
 - 5.1. *PET: EMI from RF Coils*
 - 5.2. *MR: EMI from PET Front-End Electronics*
 - 5.3. *PET: Gradients Effects on PET Front-End Electronics*
 - 5.4. *MR: Susceptibility Artifacts caused by PET Materials*
6. *Experimental Proof-of-Principle Prototypes*
7. *Summary/ take-home message*

Why simultaneous PET-MRI?

- Powerful technique for basic biomedical research and pre-clinical studies with small-animal models
- Advantages of multimodality imaging and potential benefits over PET-CT

PET-CT

- anatomical and metabolic mapping
- additional ionizing radiation dose
- image co-registration for sequential scanning

----- vs -----

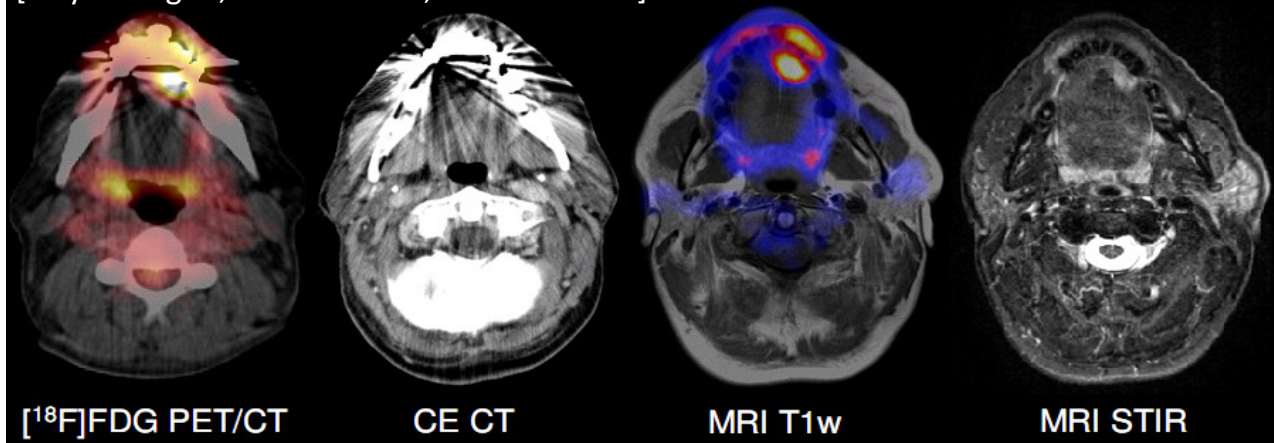
PET-MRI

- high spatial resolution
- very high soft tissue contrast
- no additional radiation dose
- simultaneous data acquisition

Relevant Challenges ...

- **Hardware: Electromagnetic Compatibility**
- Software: MR-based Attenuation Correction
- Space Constraints
- Cost Effectiveness (M€ ??)
- Ultimate Clinical Goal / Killer Application

[Sibylle Ziegler, IEEE NSS-MIC, Valencia 2011]



H. SADROZINSKI, Particle Detector Applications in Medicine (VCI 2013, Plenary/ Introductory talk)

U. Mahmood, R. Weissleder, Molecular Imaging, Radiology 219(2):316-333, 2001

B. Pichler et al, Pre-clinical PET/MR: technological advances and new perspectives in biomedical imaging, Eur J Nucl Med Mol Imaging 36 (S1), 2009

PET/MR Mutual Electromagnetic Interference

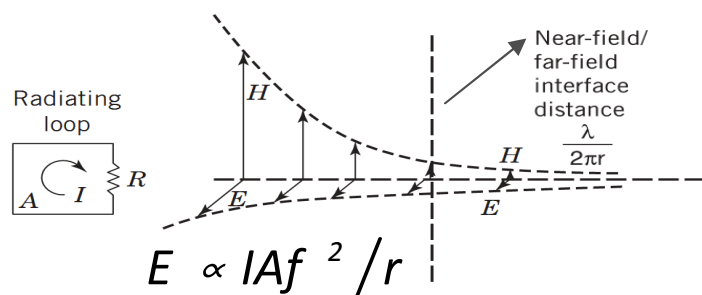
Interference on PET: static magnetic field (7T), pulsed RF, switching magnetic field gradients

- Photo-detectors (APDs, SiPMs) are insensitive to B0
- Electromagnetic Interference from pulsed RF Power†
- Induced eddy-current by the time-varying magnetic fields gradients††
- Lorentz forces on electrical conductors parallel magnetic field $\vec{F} = I \int d\vec{\ell} \wedge \vec{B}$

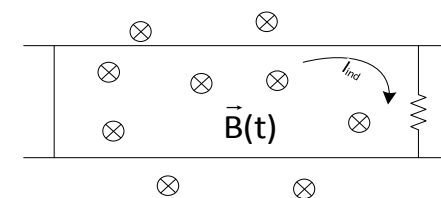
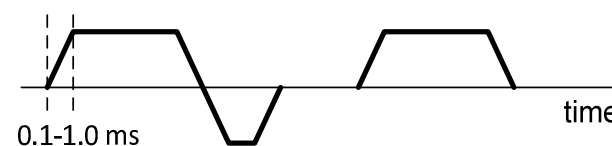
Interference on MR: magnetic susceptibility of PET materials, RF interference, loss of SNR

- Required highly homogeneous B0 (few PPMs) to avoid image susceptibility artifacts
- MRI signal is very low: more susceptible to contaminated high-frequency digital signals from PET
- EMI should be minimized -> loss of SNR -> loss of MRI sensitivity

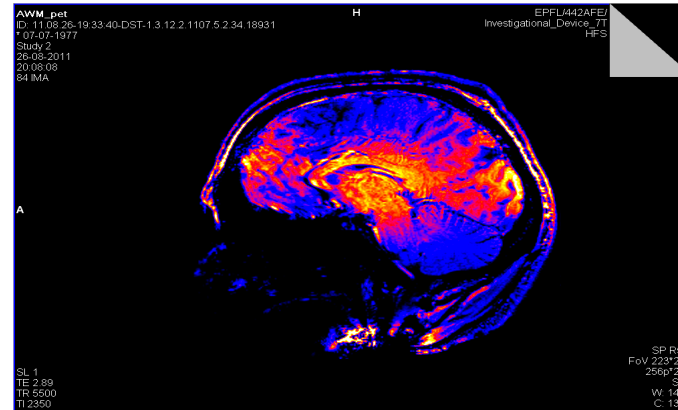
† Radiated fields from current loops



†† switched gradient fields $\vec{B}(r,t)$



$$\text{Faraday's law: } \epsilon^{ind} = -\frac{\partial \Phi}{\partial t} = -\frac{\partial}{\partial t} \int \vec{B}(t) \cdot d\vec{S}$$



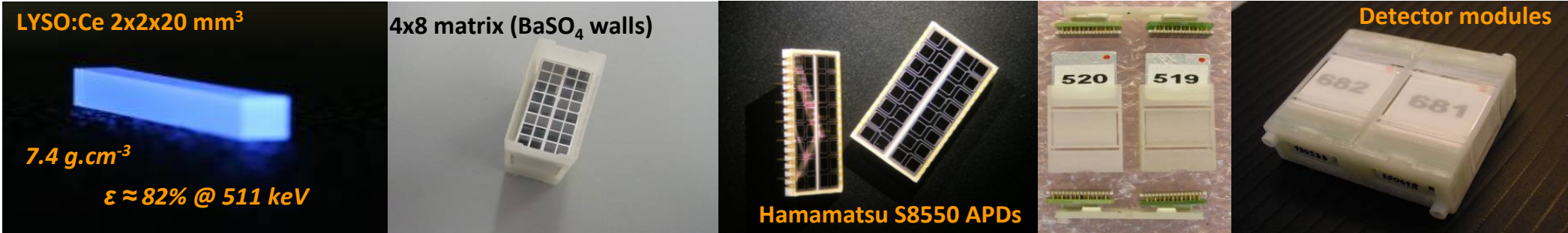
Ultra High-Field Magnetic Resonance Imaging

$$f_0 = \gamma B_0 = \sim 300 \text{ MHz @ } 7 \text{ T}$$

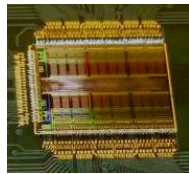
A. vom Endt, R. Gruetter R, et al. A high-performance head gradient coil for 7T systems. Proc Intl Soc magn Reson Med 15: 451, 2007



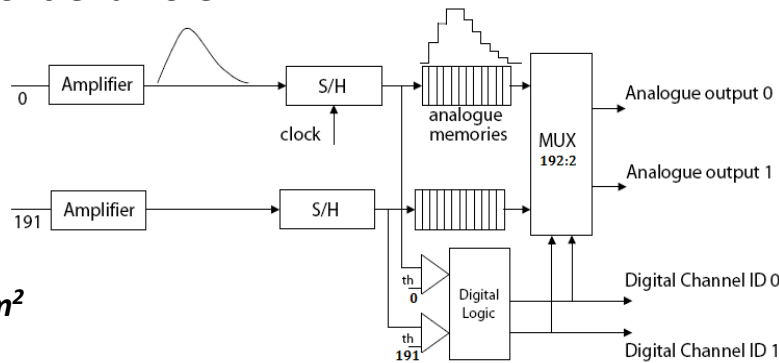
- Experimental EMI/EMC tests were carried out at the EPFL 7 Tesla magnet, Lausanne, Switzerland
- Actively shielded 7 Tesla - 68 cm bore head-only magnet (Magnex Scientific, Oxford - UK)
- Actively shielded head gradient coil
 - 36 cm inner diameter
 - 80 mT/m maximum gradient strength
 - 700 mT/(m.ms) **maximum slew rate !!!**



ClearPEM Front-end ASIC



AMS 350 nm CMOS, 70 mm²



- Input: 192 APD readout channels (~30fC input charge)
- Output: 2 highest channels (192:2 mux) -> Compton event readout
- Low noise amplifiers, pulse shaping & analog pipeline memories
- Clock frequency 50-100 Mz
- Power: 3.6 mW/channel

E. Albuquerque et al, Nucl. Instr. and Meth. A 598, pp. 802-814, 2009

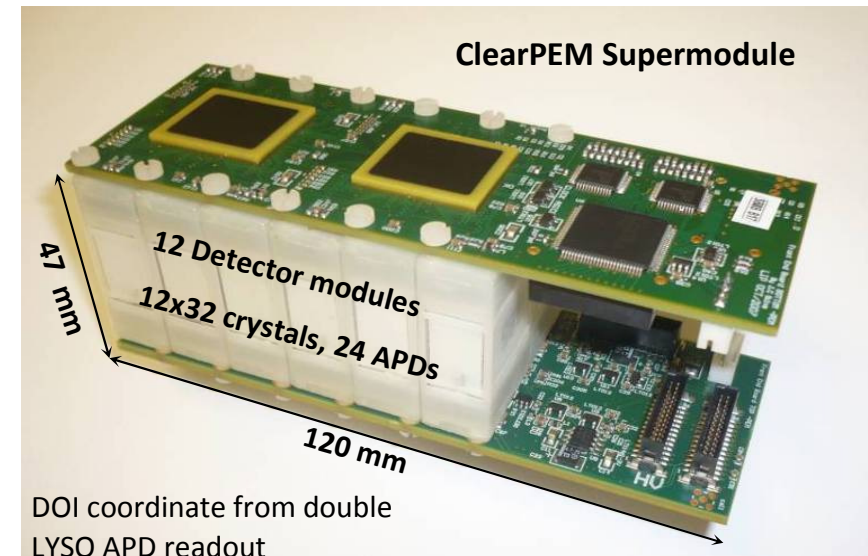
Latest developments @ LIP (FP7 EndoTOFPET-US Project)

M. Rolo et al, TOFPET ASIC for PET Applications, JINST, 2013

64-channel ASIC for SiPMs (IBM 130nm CMOS)
(see also next talk by B. FRISCH)

ClearPEM Front-end Electronic Boards

- 2x Front-end ASICs (50 MHz)
- 2x free-sampling dual 10-bit ADC (50 MHz)
- 1x LVDS ChannelLink transmitter (2.4 Gbps)

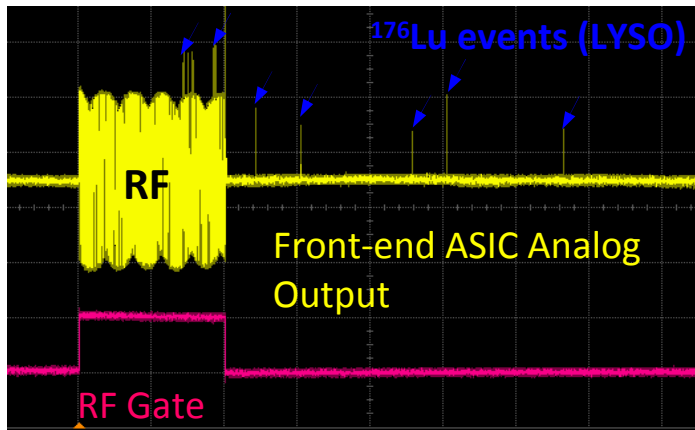


DOI coordinate from double LYSO APD readout

5.1. PET: EMI from RF Coils

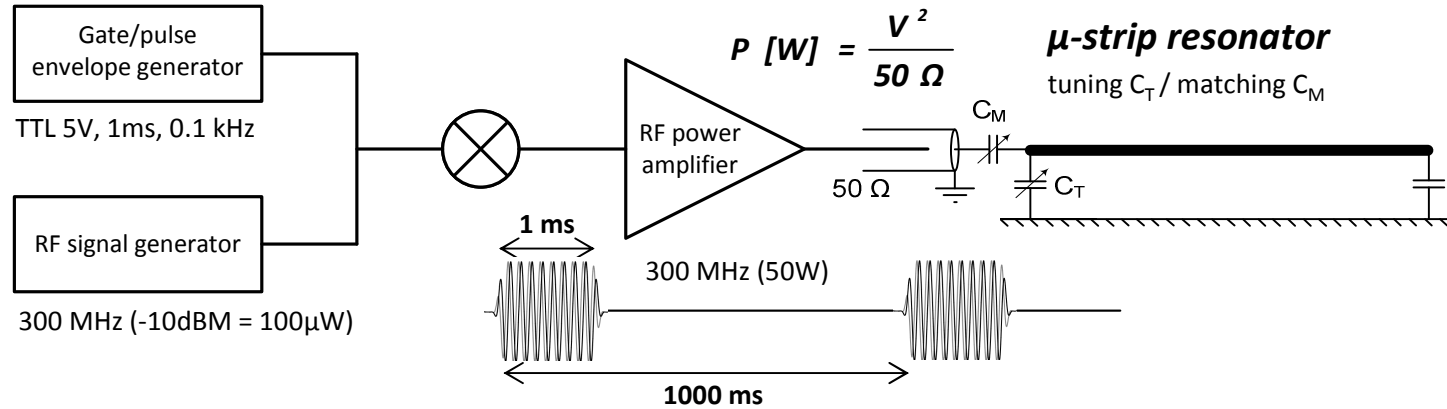
1st approach : **Low RF Power (<50W) @ RF LAB**

- Pulsed RF tolerance of the front-end electronic boards was assessed as function of the RF Power



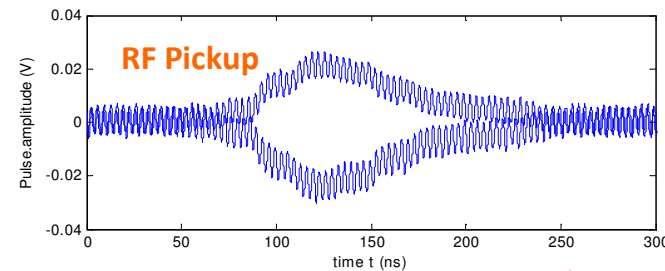
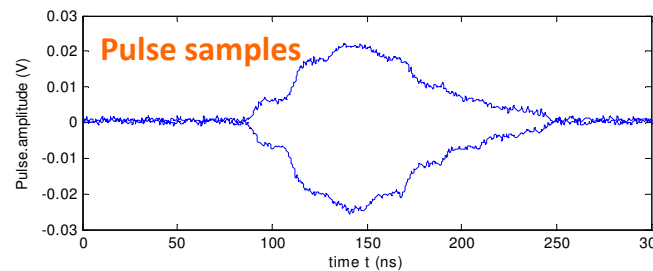
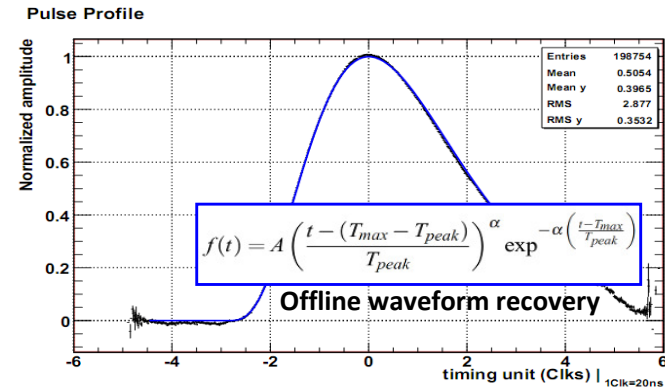
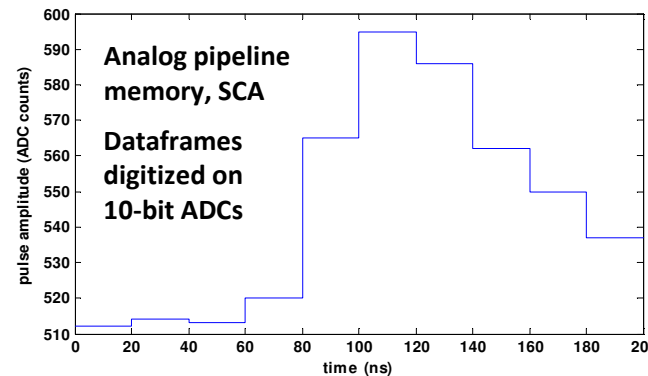
- RF pick-up (297MHz@7T) was observed on each LVDS analog output of the front-end ASIC. **No EMI shielding was used!**

- For a RF power < 50W, the LVDS analog output of the ASIC tends to reject low-amplitude common-mode RF noise pick-up.



$$P [W] = \frac{V^2}{50 \Omega}$$

µ-strip resonator
tuning C_T / matching C_M



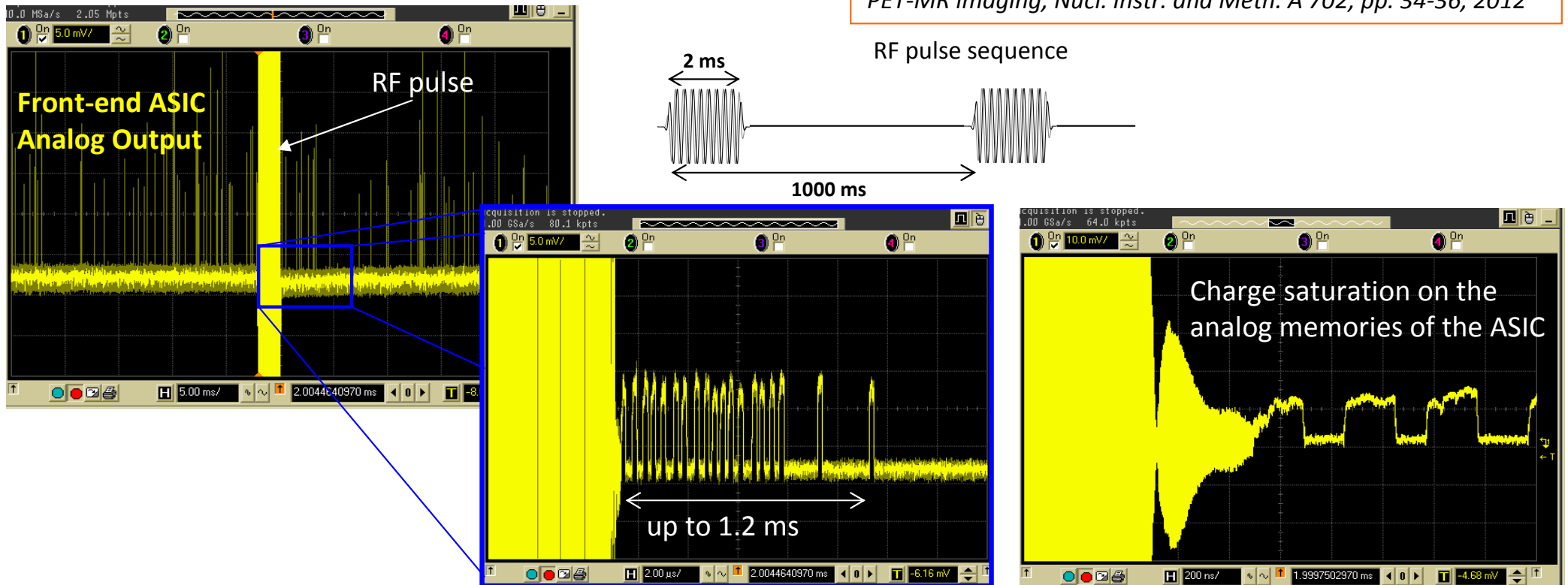
297MHz ^1H (7T)
resonance frequency

5.1. PET: EMI from RF Coils

2nd approach : High RF Power (up to 2.8 kW) @ 7T magnet RF Power Amplifiers

- Pulsed RF tolerance of the front-end electronic boards was assessed as function of the RF Power

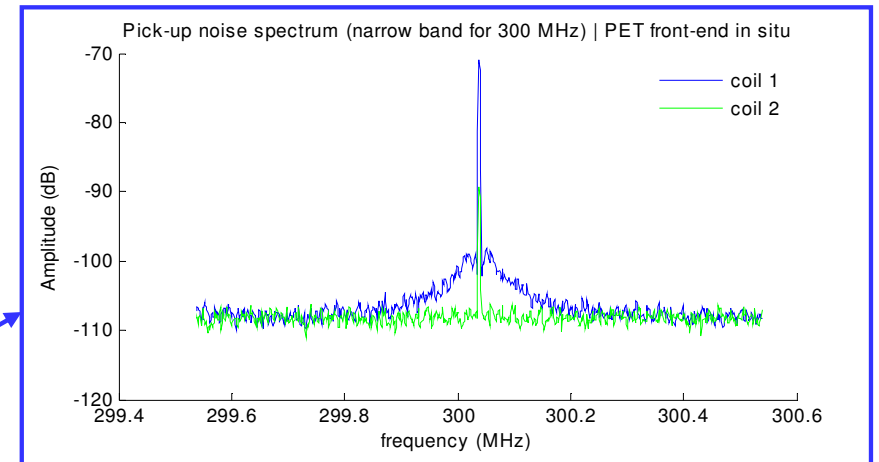
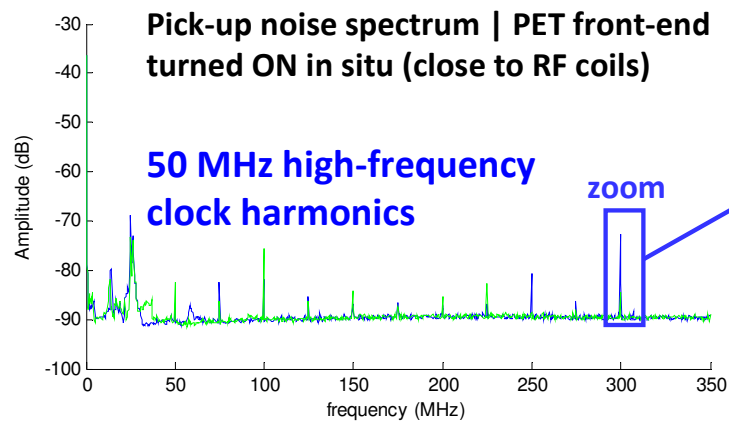
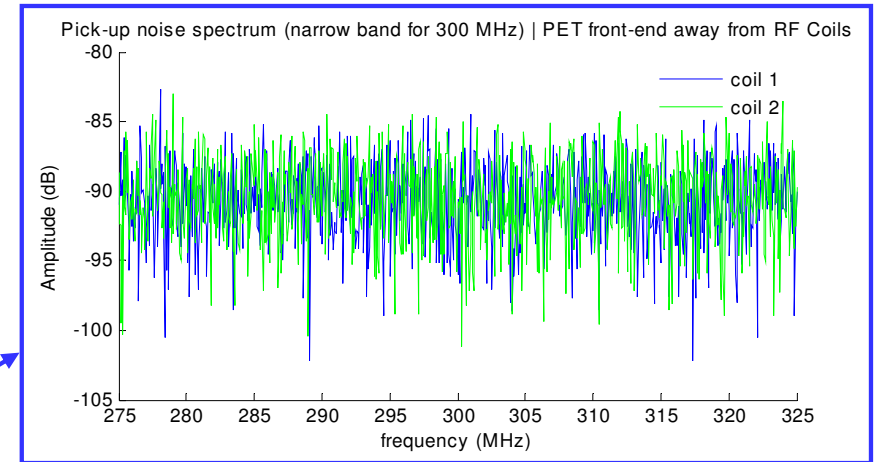
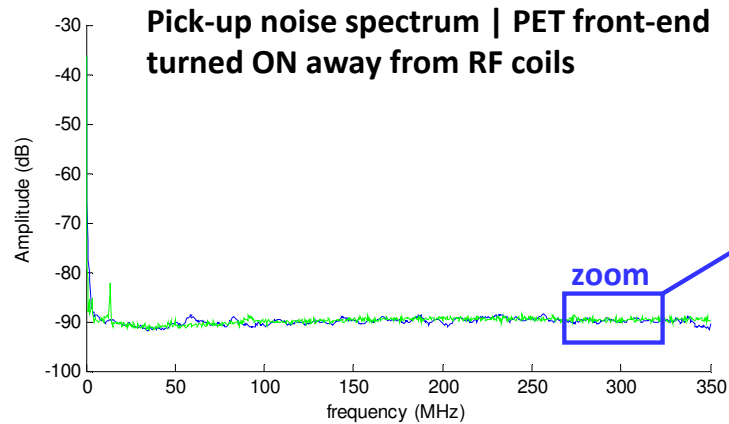
J. A. Neves et al, Feasibility and electromagnetic compatibility study of the ClearPEM front-end electronics for simultaneous PET-MR imaging, Nucl. Instr. and Meth. A 702, pp. 34-36, 2012



- At a maximum RF power = 2.8kW, we have observed a saturation of the front-end ADCs dynamic range during the RF pulse, and a self-triggering state induced by *RF eddy-currents* that create a burst of events remaining over 1.2 ms after the RF pulse. **No EMI shielding was used!**

5.2. MR: EMI from PET Front-End Electronics

1st approach : Spectrum Analyzer measurements

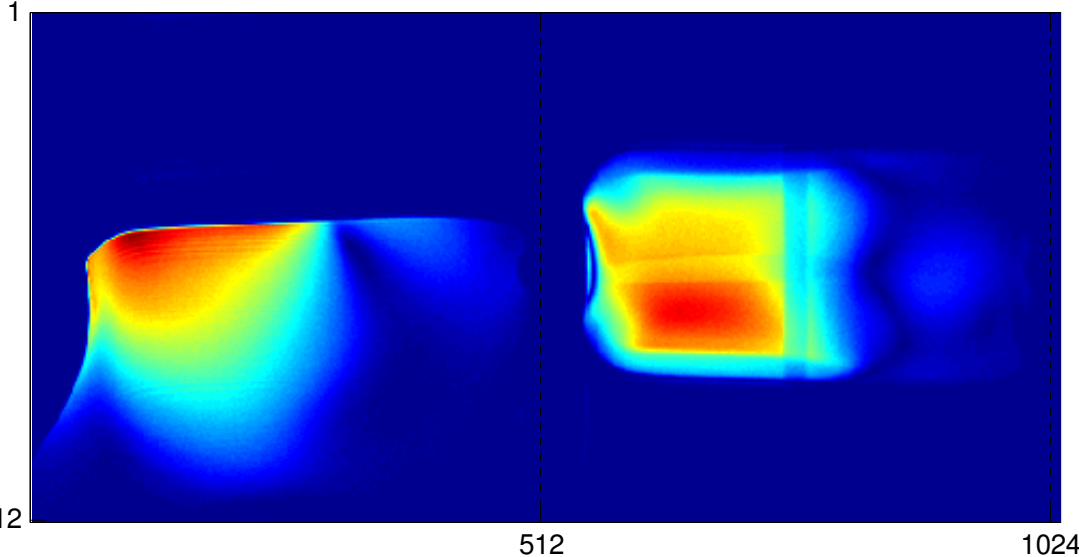


- Noise pick-up measurements with PET front-end electronics close to the RF coils shows an important EMI contribution from digital electronics. No EMI shielding was used!
- The 300 MHz harmonic from the 50 MHz system Clock was detected to enter in the narrow dynamic range of the RF preamplifiers, being responsible for the noise propagation into the RF receiver chain (SNR degradation)

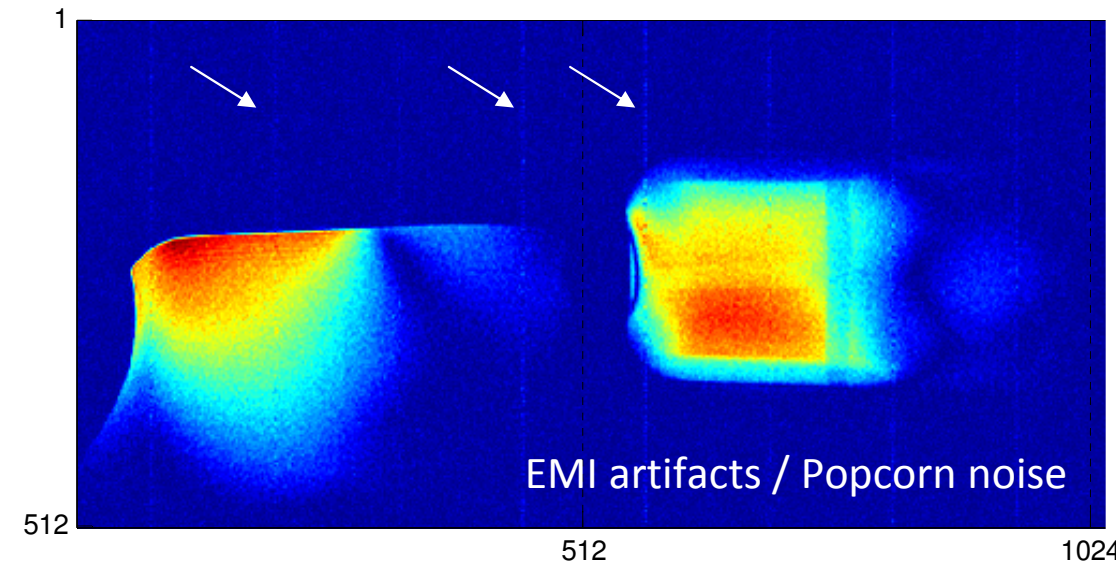
5.2. MR: EMI from PET Front-End Electronics

2nd approach : Analysis of pick-up noise on acquired MR images

RF Coil + PET Front-end OFF



RF Coil + PET Front-end ON



- MR images from a water-filled phantom were acquired with a surface RF coil with the PET front-end electronics in its vicinity turned OFF and turned ON. No EMI Shielding was used!
- Coherent results with Spectrum Analyser measurements showing the contribution of high-frequency Clock harmonics propagated into the RF receiver chain
- A shift on the system Clock frequency from 50 to 52.5MHz was proposed to eliminate pick-up noise from the front-end digital electronics

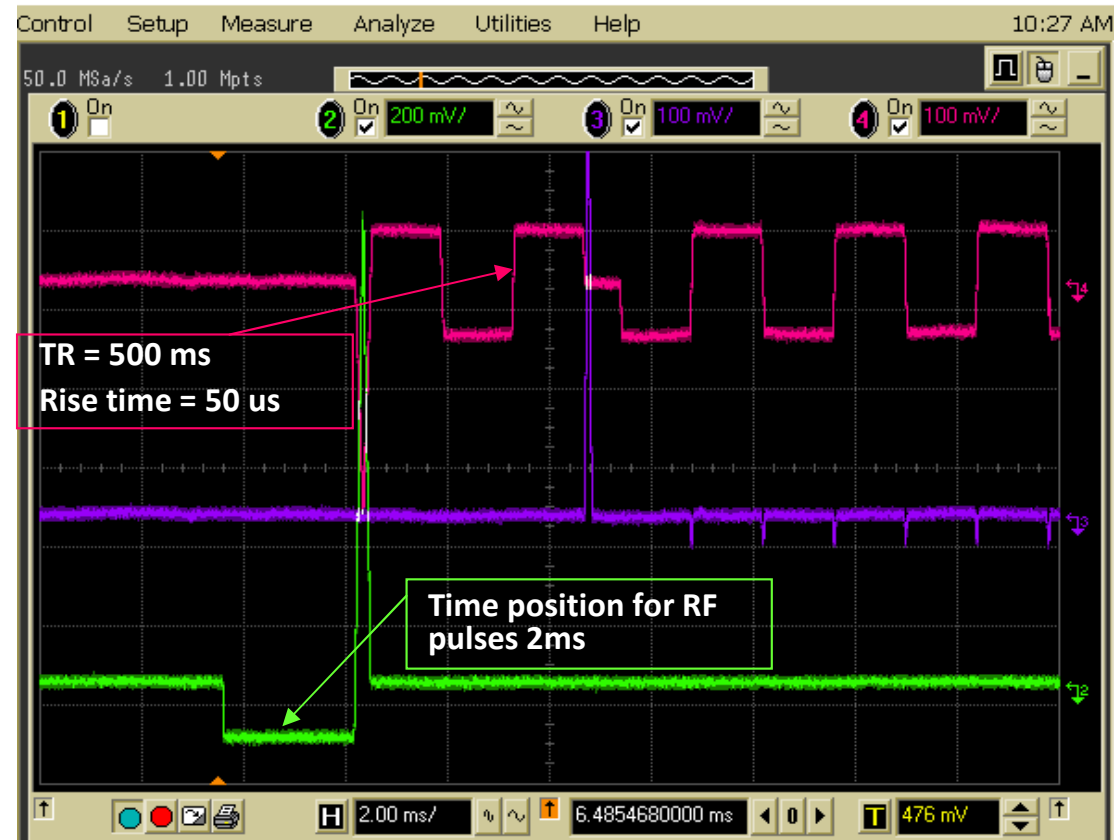
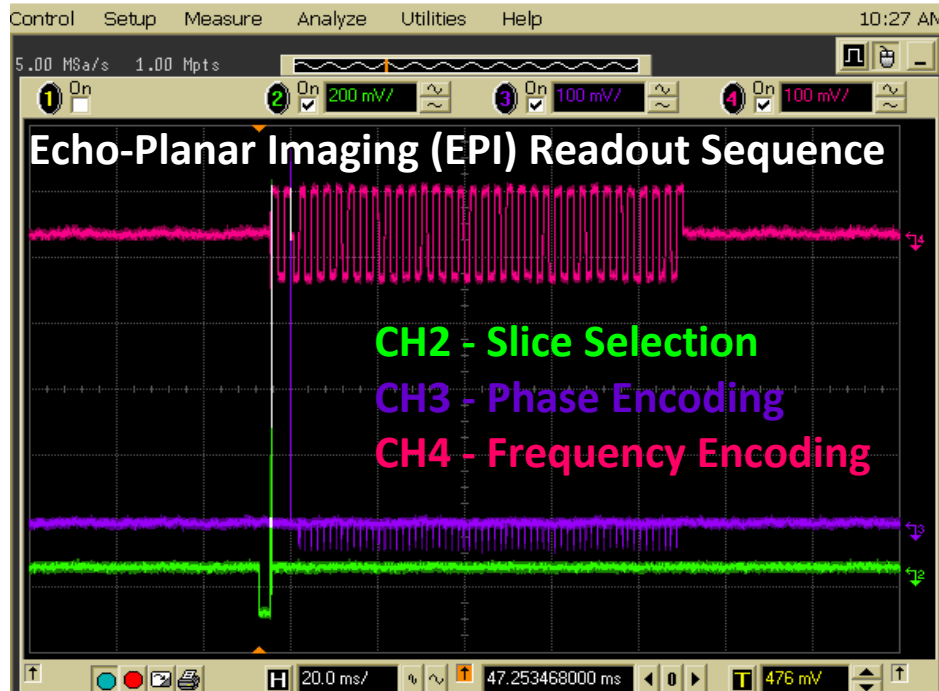
5.3. PET: Gradients Effects on PET Front-End Electronics

Magnetic Field Gradients: linearly varying magnetic fields applied in addition to the main magnetic field B0 to achieve spatial encoding

$$G_x = \frac{dB}{dx}, G_y = \frac{dB}{dy}, G_z = \frac{dB}{dz}$$

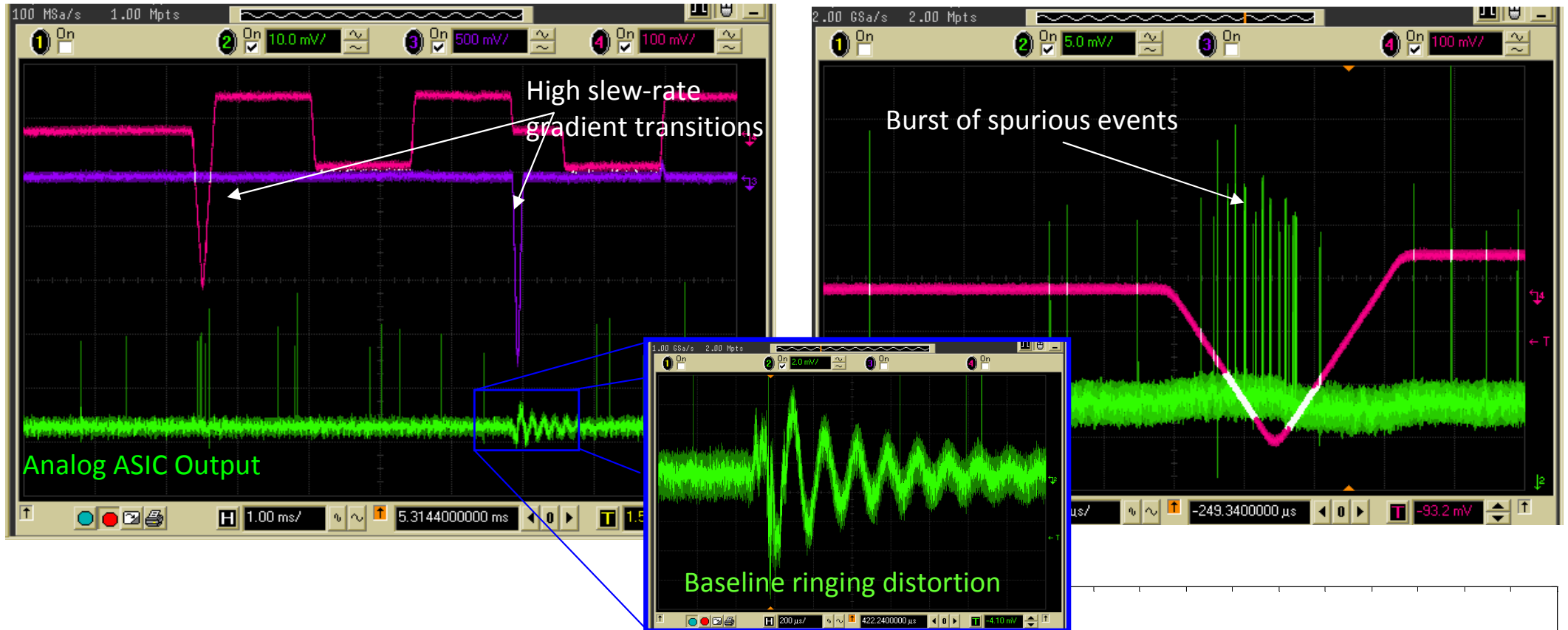
EPFL 7T magnet - Actively shielded head gradient coil

- 80 mT/m maximum gradient strength
- 700 mT/(m.ms) **maximum slew-rate !!!** $\frac{dB}{dxdt}$

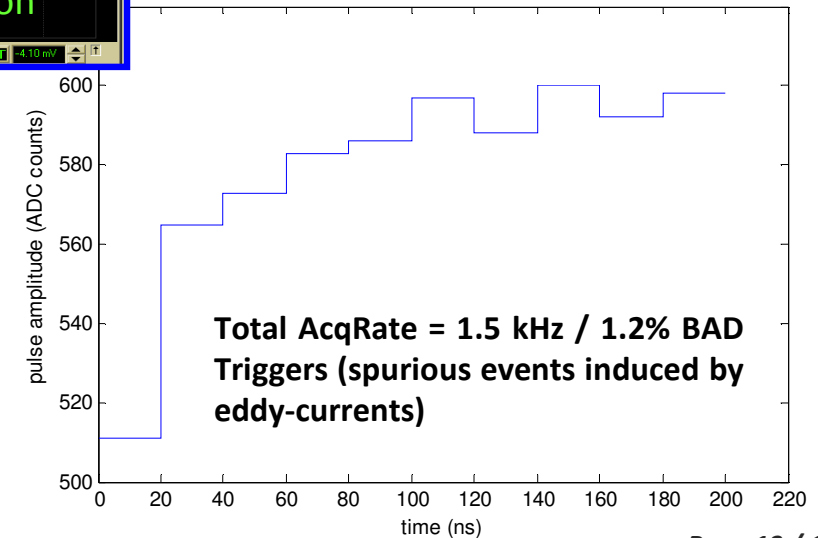


- Gradients effects on front-end electronics were studied with a EPI sequence

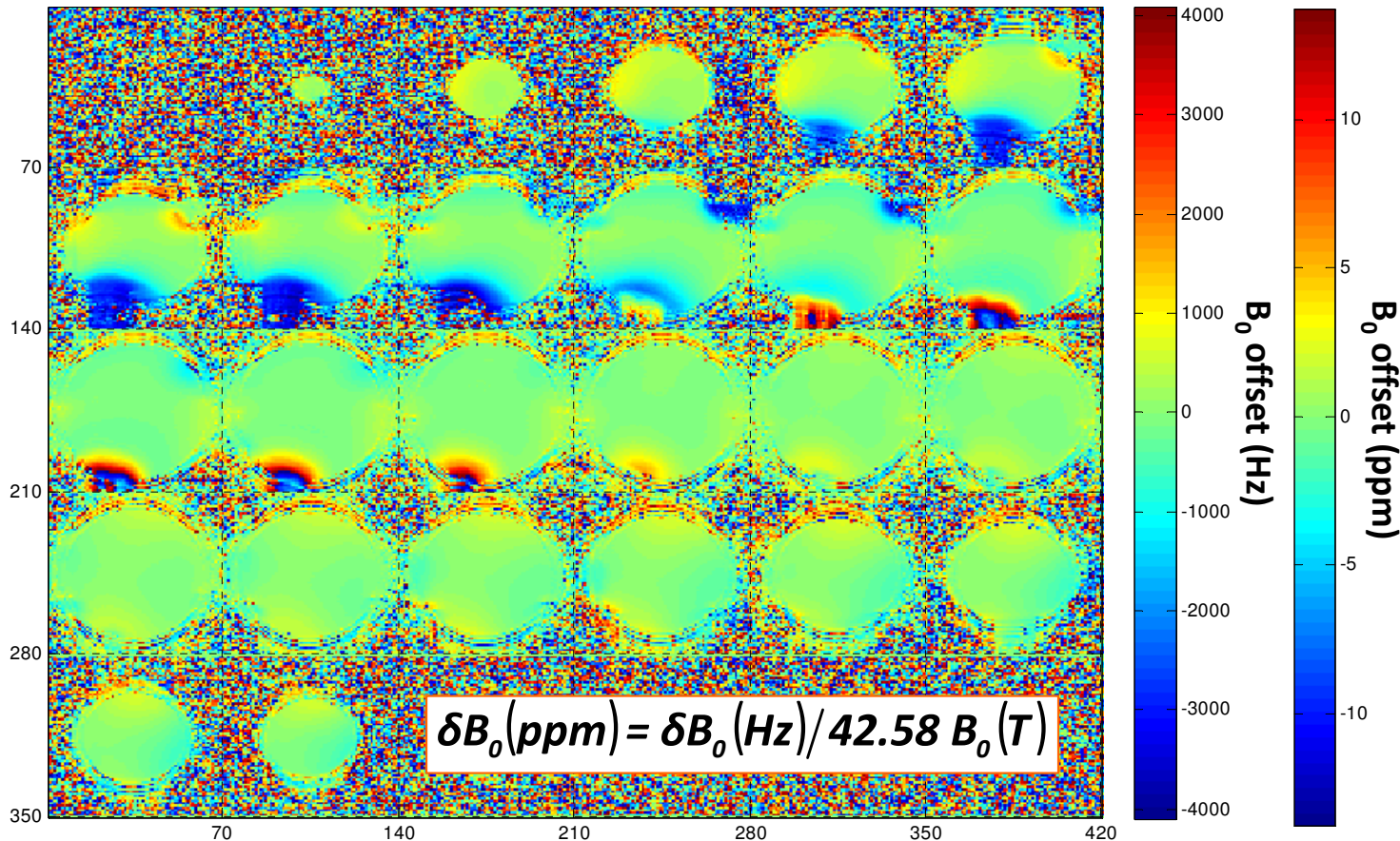
5.3. PET: Gradients Effects on PET Front-End Electronics



- High slew-rate gradient transitions were found to be responsible for induced *eddy-currents* on front-end boards power/ground planes which causes ASIC baseline distortions and bursts of spurious events with a characteristic saturated/ flat waveform
- the expected time scale for the eddy-currents is compatible with the exponential decay time of the ringing distortion of the ASIC baseline (~600us)



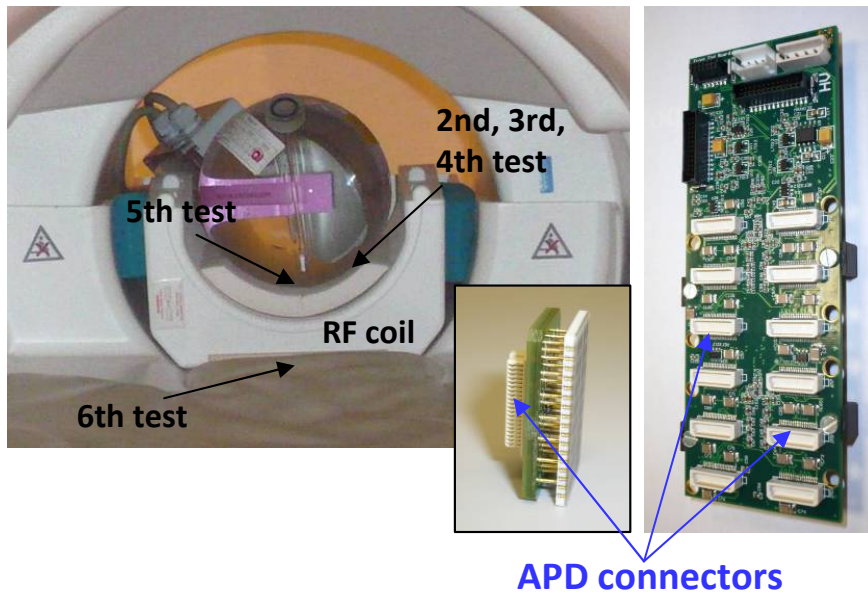
5.4. MR: Susceptibility Artifacts caused by PET Materials



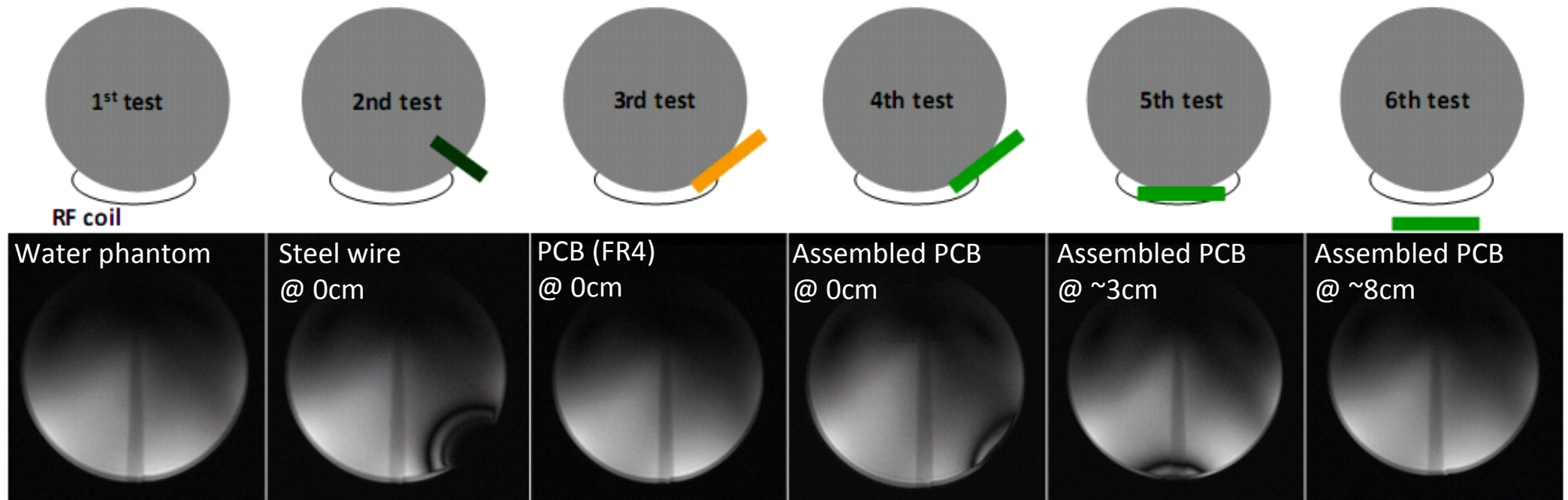
J. F. Schenck, The role of magnetic susceptibility in magnetic resonance imaging, Med. Phys. 23 (6), 1996

- B0 field phase-difference mapping (susceptibility image)
- The ClearPEM module was placed close to a oil-filled spherical phantom (~25 cm diameter) inside a head coil
- B0 field distortions below 10 ppm were observed over an extension of 5 cm

5.4. MR: Susceptibility Artifacts caused by PET Materials



- B0 field distortions caused by front-end board materials were also evaluated by the homogeneity analysis of a water-filled spherical phantom (~25 cm diameter)
- A ClearPEM front-end board was positioned in different points to assess its influence on B0 distortion
- Nickel plated APD connectors were found to be responsible for the observed B0 field lines distortions

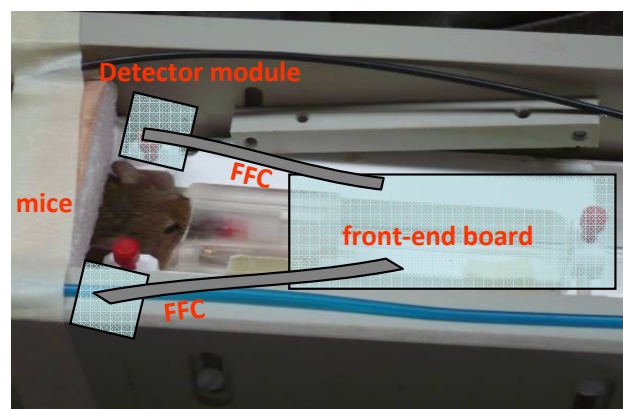




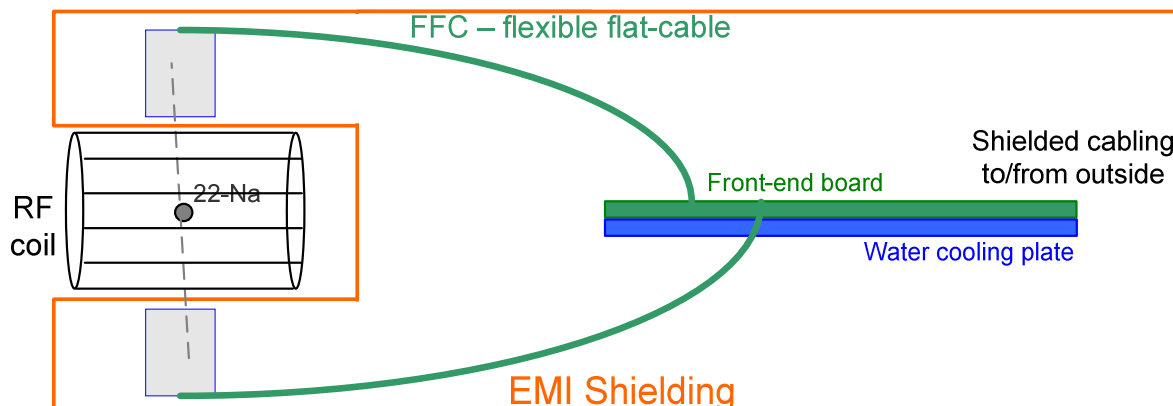
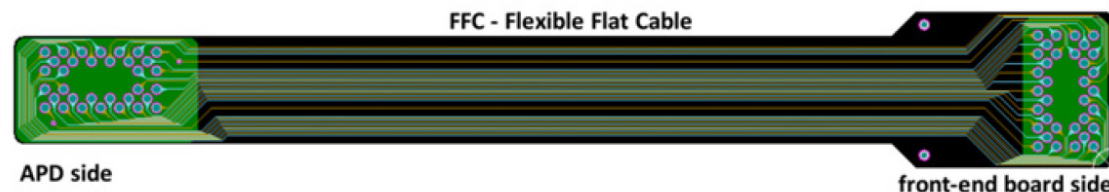
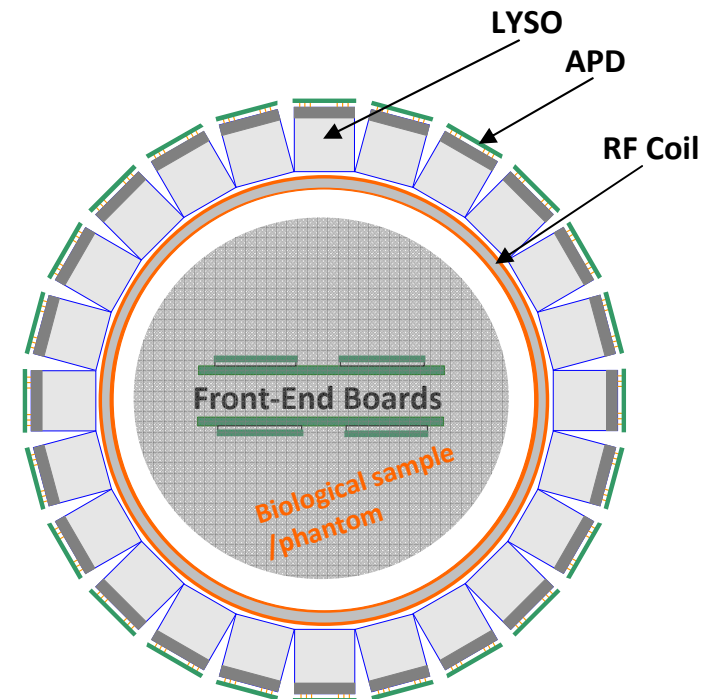
Small-Animal 9.4 T



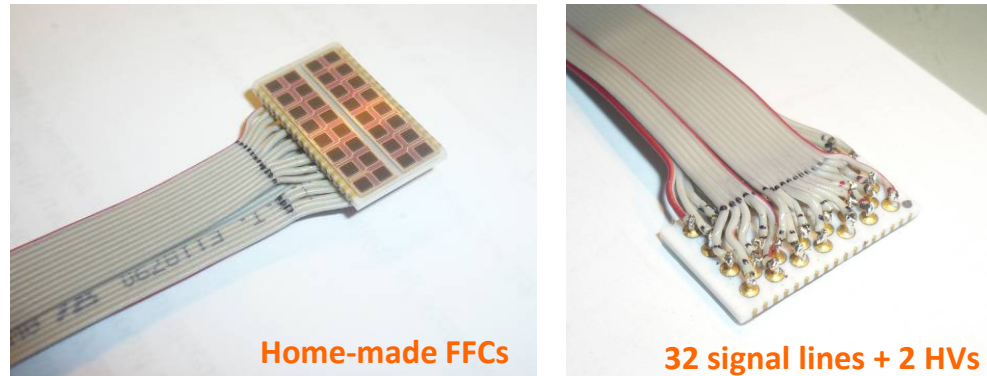
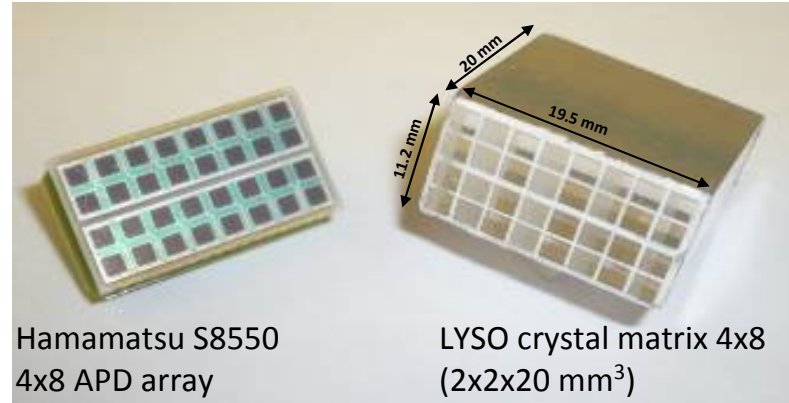
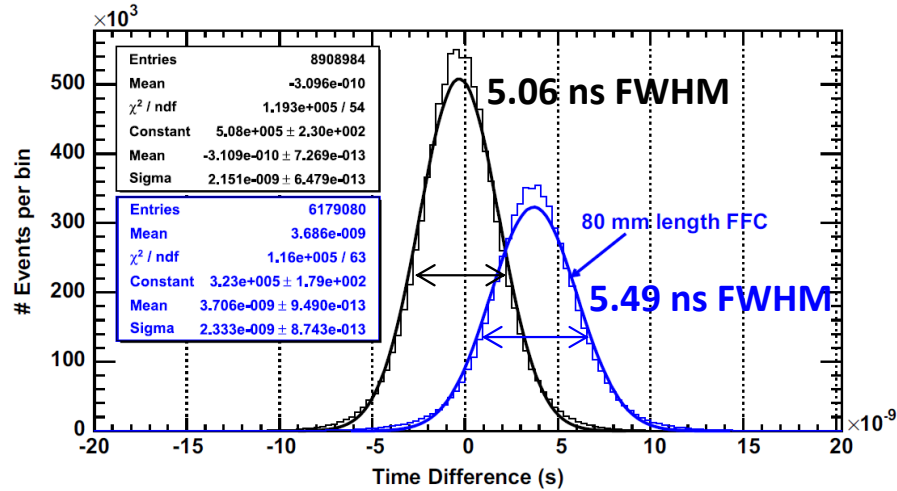
Small-Animal 14.1 T



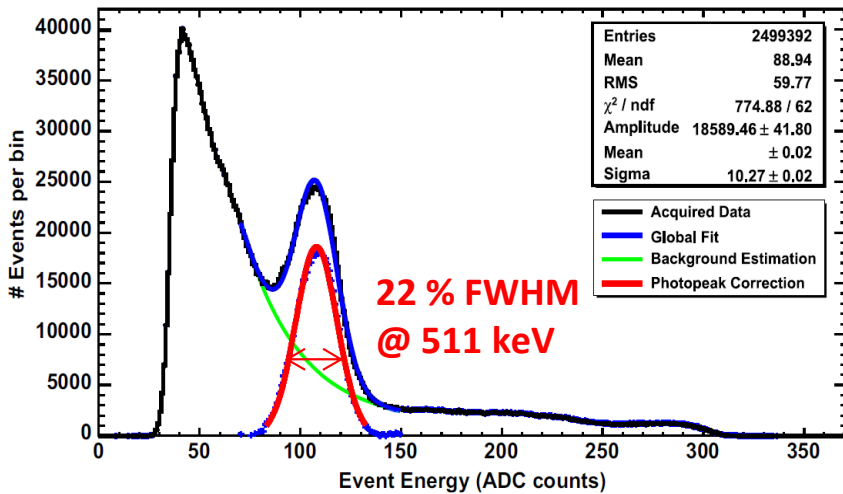
- Small-animal PET insert for UHF PET-MR
- Detector ring of 12 or 24 APD+LYSO modules
- <math><140\text{ mm}</math> outer \varnothing / $85\text{ mm}</math> inner $\varnothing$$
- Axial FOV = 19.5 mm
- LYSO crystals matrices in single-ended scintillation light readout mode
- APD charge signals transmitted to the front-end ASIC by via flexible flat-cables ($\sim 150\text{ mm}$ length)



Small-animal PET insert for UHF PET-MR



APD-coupled flexible flat-cable for
LYSO scintillation light readout

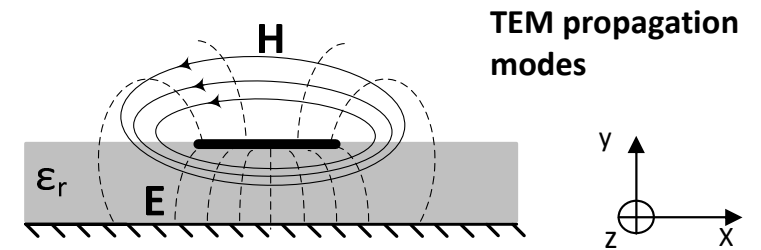


J. A. Neves et al, 9.4–14.1 T small-animal PET-MR imaging: Feasibility analysis of LYSO APD readout via long signal lines, Nucl. Instr. and Meth. A 702, pp.98-100, 2012

Non-significant degradation on Time and Energy Resolution was observed with the FFC introduction

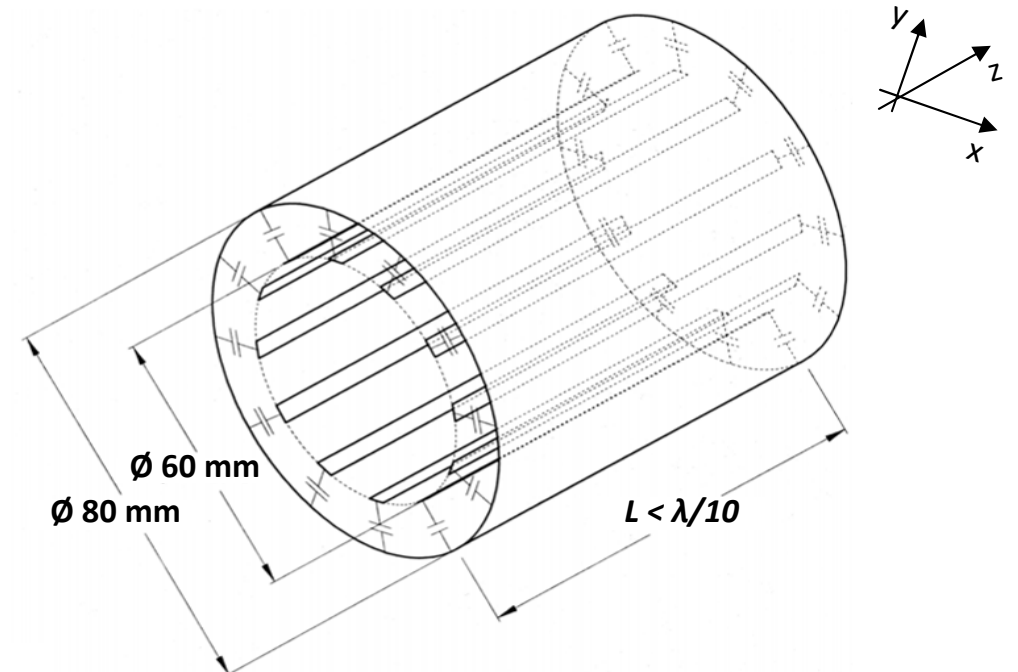
RF Coil Design: Coupled Microstrip Line Transverse Electromagnetic (TEM) Resonator

- Microstrip TEM resonator: best compromise for UHF (≥ 7 T)
- 8 Conductor elements (copper 38 μm thick)
- Air/ PMMA dielectric substrate
- Cylindrical shield (current return paths)
 - Segmented shielding at lower frequencies (kHz range)
 - to block the propagation of eddy currents induced by the switching magnetic field gradients
 - Continuous RF shielding at high-frequency (MHz range)
- 2 Driving elements in 'quadrature'
- Mutual inductive coupling between elements
- Matching to 50 Ω and individual tuning to 297.2 MHz (7T)
- FDTD/ FEM Electromagnetic Simulation
 - CST Microwave Studio [®]
 - E/H field distribution
 - Resonant Modes
 - S-parameters/ Q-factor



$$\mathbf{E}(x, y, z) = E(x, y)e^{j(\omega t - k_z z)}$$

$$\mathbf{H}(x, y, z) = H(x, y)e^{j(\omega t - k_z z)}$$



J. T. Vaughan et al. High frequency volume coils for clinical NMR imaging and spectroscopy. Magn Reson Med, 21:206-218,1984

Acknowledgements



Ricardo Bugalho
Catarina Ortigão
Rui Silva
José C. Silva
João Varela
Stefaan Tavernier



Arthur W. Magill
Rolf Gruetter
Carole Poitry-Yamate
José P. Marques
Mayur Narsude
Wietske Zwaag



Fundação para a Ciência e a Tecnologia
MINISTÉRIO DA CIÊNCIA, TECNOLOGIA E ENSINO SUPERIOR

PhD Grant SFRH/BD/33667/2009

- MR compatibility of the ClearPEM front-end electronics was assessed by evaluating the mutual EMI mechanisms into a 7T MRI system;
- The presented results demonstrate that the front-end electronics withstands to pulsed RF power and to the strong magnetic field gradients, introducing some impact upon MR signal acquisition (careful EMI shielding needed);
- A new design for UHF small-animal PET-MR was proposed by using long flexible flat cables to transmit the APD charge signals to the ClearPEM front-end ASIC;
- Proof-of-principle prototypes are being tested;
- A new dedicated RF coil for UHF was designed intending to demonstrate the simultaneous PET-MR acquisition with minimal interference between both systems.

:) Thank you!